

Simulation of Detector Background Due to Beam Halo in RHIC

A. J. Stevens

October 1997

Collider Accelerator Department
Brookhaven National Laboratory

U.S. Department of Energy

USDOE Office of Science (SC)

Notice: This technical note has been authored by employees of Brookhaven Science Associates, LLC under Contract No. DE-AC02-76CH00016 with the U.S. Department of Energy. The publisher by accepting the technical note for publication acknowledges that the United States Government retains a non-exclusive, paid-up, irrevocable, world-wide license to publish or reproduce the published form of this technical note, or allow others to do so, for United States Government purposes.

DISCLAIMER

This report was prepared as an account of work sponsored by an agency of the United States Government. Neither the United States Government nor any agency thereof, nor any of their employees, nor any of their contractors, subcontractors, or their employees, makes any warranty, express or implied, or assumes any legal liability or responsibility for the accuracy, completeness, or any third party's use or the results of such use of any information, apparatus, product, or process disclosed, or represents that its use would not infringe privately owned rights. Reference herein to any specific commercial product, process, or service by trade name, trademark, manufacturer, or otherwise, does not necessarily constitute or imply its endorsement, recommendation, or favoring by the United States Government or any agency thereof or its contractors or subcontractors. The views and opinions of authors expressed herein do not necessarily state or reflect those of the United States Government or any agency thereof.

RHIC PROJECT

Brookhaven National Laboratory

**Simulation of Detector Background Due to
Beam Halo in RHIC**

A. J. Stevens, P. A. Thompson, D. Trbojevic

October 1997

Simulation of Detector Background Due to Beam Halo in RHIC

A. J. Stevens, P. A. Thompson, D. Trbojevic

I. Introduction: Beam Halo and Description of Methodology

So called “machine background” in a detector is dominated by beam-gas interactions and the interaction of “beam halo” particles near the detector. The latter particles are generated by small angle disturbances such as beam-gas elastic scattering and the presence of high order resonances which causes a diffusive growth of betatron amplitude. For some beam particles a betatron amplitude is reached which is greater than the dynamic aperture of the machine, after which the growth will accelerate until some physical aperture is encountered. When such apertures are directly upstream of detectors, significant background can result.

The first measure of defense against such background is a limiting aperture collimator. In the limit of infinitely slow halo growth, the halo particles will always strike such a collimator. In this limit halo detector background is caused by particles which *elastically outscatter* from the collimator and interact close to the detector. The efficiency of the collimator¹ is therefore a significant issue.

One simple measure of halo background in a detector is the single hit rate which, of course, depends on location within the detector. A background flux (hits per cm² per sec.) can in general be written as:

$$(1) \quad Flux = N \times (1 - \epsilon) \times P \times F$$

where N is the number of particles per unit time on the collimator, $(1-\epsilon)$ the collimator inefficiency, P the fraction of outscatters interacting “locally” and F the secondary particle fluence per locally interacting particle (hits per cm² per local interaction).

The remainder of this note is primarily concerned with summarizing the work that has been done to date in estimating the components of Eqn. (1). Section II below describes the simulation of halo growth and evaluation of the collimator efficiency. Section III describes tracking studies through the RHIC lattice of the outscattered particles (estimation of P), and Section IV hadron cascade calculations performed to estimate F . Finally, Section V makes an upper limit estimate for N , and compares the halo background estimate to simulations of beam-gas background.

¹ The efficiency is defined as the fraction of incident particles which interact inelastically.

II. Simulation of Halo Growth and Outscattering

As mentioned in the preceding section, halo growth begins when some disturbance increases a particle's betatron amplitude such that the transverse motion is beyond the dynamic aperture of the machine. Although in principle simulation might begin with the disturbances, in practice what disturbances are important is unknown, at least until the machine exists.² A much simpler algorithm was adopted which increases betatron amplitude, in only one dimension, based on measurements made at the SPS [1]. Specifically, a parameterization of these measurements was adopted which characterizes the change in amplitude $a(a = \sqrt{\epsilon})$ per second as:

$$(2) \quad \delta a (\text{root meters} / \text{sec}) = 2.45 \times \sigma \times \exp\left(\frac{a}{\sigma} - 4\right)$$

$$\text{where } \sigma = \sqrt{\frac{\text{Emittance}}{6\beta\gamma}}$$

Thus the dynamic aperture is assumed to be 4σ . For the numerical results given in this note the emittance for Au ions (at 100 GeV/u) and protons (at 250 GeV) is assumed to be 40 mm-mrd and 20 mm-mrd respectively. It should be clear that the assumption that the SPS measurements are descriptive of the halo growth that will exist at RHIC is **not** well justified.

A simple FORTRAN program was written which samples orbits at the front edge of a 45 cm. long horizontal collimator. For the numerical results given in this note the collimator was assumed to be 4m into one of the "long straight sections" with its edge at 5.5σ from the beamline. Each orbit is initially assigned an amplitude slightly above 4σ and a random phase. The transverse position is then evaluated once per revolution to see if has encountered either the front edge or face of the collimator. If it has not, the amplitude grows more according to Eqn. (2) and another revolution time step is taken. The output of this program is a file of positions and angles of orbits encountering the collimator.

The particles are then transported through the collimator by another Monte Carlo program written by Van Ginneken. [2]. Orbits which have not inelastically interacted are the outscatters described in Section I above. Another file of the parameters of these is generated for tracking through the lattice as described in the next Section.

The 5.5σ assumption deserves some explanation. If the collimator is placed at a large distance from the start of the dynamic aperture, then according to Eqn. (2), the amplitude is increasing very rapidly per revolution at the time when it is large enough to encounter the edge of the collimator. However, the phase may be "wrong" at this time, and the probability that some other physical aperture is encountered is now quite significant since the slow growth assumption described in Section I is now violated. Furthermore, the additional implicit assumption has been made that the distance between the limiting aperture collimator and the next closest aperture is at

² Intrabeam Scattering is a major source of beam loss for heavy ions but, to date, tracking studies have showed this to be a loss in longitudinal phase space.

least the distance that the halo would grow in $O(\sim 10^2)$ orbits. This is believed to be the time required for horizontal-vertical coupling which is necessary for the single one-dimensional scraping described here to be effective.³ It should be clear that quantitatively Eqn. (2) should not be taken seriously. However it is also clear qualitatively that the scraper must be “close to” the good beam and that there exists a “significant distance” between the limiting aperture collimator and other apertures.

The single pass⁴ “scraping inefficiency” as a function of species (Au ions or protons), alignment, and crossing point β^* value is shown in Fig. 1. The following characteristics are noted:

- (1) The inefficiency is much lower for Au than for protons. This follows from the inelastic cross section being much higher for the ions and from the fact that the ions multiple-scatter much less per unit path length while in the collimator material.⁵
- (2) There is extreme sensitivity to the collimator tilt (and hence required flatness). This follows from the magnitudes of the quantities involved given the slow growth parameterization. The situation is illustrated in the sketch shown in Fig. 2. In the approximation that the collimator is in a dispersionless region and that any variation of the beta function over the length of the collimator is ignored, then maximum scraping efficiency occurs when the “beam” is parallel to the collimator face, i.e., when the tilt is given by $-\alpha X/\beta$. Otherwise one is “clipping” the collimator edge as illustrated in Fig. 2. Now the parameters adopted for this simulation give an average value for δX (See Fig. 2) of about **5 microns**, from which the sensitivity for a 45 cm. long collimator directly follows. The mis-alignment illustrated in Fig. 1 is in the worst case direction which corresponds to the back end of the collimator being too close to the beam line. The opposite direction mis-alignment is about 1/3 of the loss of efficiency shown in Fig. 1.
- (3) There is some sensitivity to the β^* value. This follows from the growth model which increases the amplitude some amount per revolution. Since the corresponding transverse distance increase (at constant phase) is $\sqrt{\beta_H}$ times this (where β_H is the horizontal beta function at the collimator which varies inversely with β^*), δX (see Fig. 2) will be larger and the efficiency higher for a larger β_H . (The scale on Fig. 1 may be somewhat misleading in the case of optimum alignment for Au where the inefficiency increases by a factor of 3 between $\beta^* = 1\text{m}$ and $\beta^* = 10\text{m}$.)

Now in the “real world”, alignment well below 25 μrad . (or perhaps *effective* alignment when fill-to-fill reproducibility is considered) will not be achievable. The conclusion of this

³ G. Parzen, private communication. In general the dynamic aperture is smaller in the horizontal plane.

⁴ Some outscattered particles will interact on the collimator in subsequent turns.

⁵ The collimator has been assumed to be a nickel-copper compound.

Section is therefore that inefficiencies of 0.05 for Au ions and 0.50 for protons are reasonable estimates.

III. Tracking Through the Lattice

To date, only Au outscatters have been tracked through the lattice using the tracking program TEAPOT [3]. Both collimators (one for the Blue, or clockwise ring and one for the Yellow ring) are assumed to be downstream of the local crossing point at 8 o'clock.

Files consisting of 512 outscattered orbits (Section II above) were tracked. Fig. 3 shows the initial distributions of horizontal phase space and momentum for a file generated assuming $\beta^* = 1\text{m}$ at 8 o'clock and optimal collimator alignment. Fig. 3(b) shows that the outscattered Au ions have a significant momentum loss (compared to the bucket size of 0.2%) in the collimator material. This is due to the very high energy loss ($dE/dx \sim Z^2$) for ions and does not reflect the situation with protons.

The loss pattern of outscattered particles is strongly dependent on the machine set up. Those interaction regions tuned for low β^* have apertures upstream of the crossing point which are effectively small compared to regions with relatively high β^* . It is believed that only 6 o'clock and 8 o'clock will be capable of running at $\beta^* = 1\text{m}$. Fig. 4 shows the loss pattern for the Blue ring for a geometry where 6 and 8 o'clock are at $\beta^* = 1\text{m}$ with the remaining IR's at $\beta^* = 10\text{m}$. The losses near the beginning of the plot occur in the dispersive section of the 8 o'clock straight section and are primarily the large off-momentum particles in Fig. 3(b). The largest losses occur at 6 o'clock (68% - mostly on the first turn) and 8 o'clock (12%) as expected. The pattern is quite similar for the Yellow ring for the same machine set-up which is shown in Fig. 5. In both cases, the 6 o'clock IR is between the collimator and 8 o'clock and suffers the most loss. For comparison with Fig. 4, Fig. 6 shows a loss pattern where the 12 o'clock tune was changed to $\beta^* = 2\text{m}$. This IR now absorbs some of the losses and with the result that the 6 o'clock losses are reduced from 68% to about 45%.

The evaluation of "P" in Eqn. (1) thus depends on what experiment is under consideration and the tune of the entire machine, so there is no single value. For the purposes of this note, the worst case value of P will be taken to be 0.5, but most IR's will be lower than this by a factor of 5.

As part of the tracking studies several locations were examined for possible secondary collimators. The best location for a secondary collimator would be a lattice location which differs in betatron phase from the "primary" collimator by about 165° [4]. Indeed the Q9-D9 region immediately downstream of the primary collimator has approximately the correct phase difference and some ($\sim 5\text{m}$) free space. The studies to date for a secondary collimator are given elsewhere [5]. An aperture at 6.5σ at this location would be expected to intercept approximately 40% of outscattered orbits which would otherwise encounter one of the $\beta^* = 1\text{m}$ interaction quads. However, as mentioned in the preceding Section, one of the requirements for the primary

collimator to be efficient is that there be a “significant distance” between the primary collimator and all other apertures. The potential usefulness of a secondary collimator may be best answered by actual machine studies when the nature of the backgrounds which are actually troublesome is more clear. It should be noted that the Q9-D9 region has another potential use; since this region has a sizable dispersion, a horizontal collimator here could set the momentum aperture of the machine.

Tracking and secondary collimator effectiveness studies for protons remain a topic for future work. The remainder of this note is therefore restricted to the consideration of Au ions.

IV. Hadron Cascade Calculations

Hadron Cascade calculations were done using the CASIM [6] and MARS [7] codes. In both cases the outscattered ions were simply treated as 197 100 GeV/c nucleons interacting in the beam pipe at the position of one of the high beta quadrupoles upstream of an interaction region. Upstream of the “detector region” approximations were made for the Q3, Q2, Q1, D0, and DX magnets which included the magnetic fields.

It is important to understand some of the differences in the two codes as well as in the simulations described here. In CASIM, hadrons are in principle created and transported properly down to ~ 50 MeV. In the calculation described here, the threshold was set to 5 MeV, but cross sections between 50 and 5 MeV are not correct. When a hadron drops below the threshold energy a very crude approximation is made to account for lower energy interactions. Due to the absence of detailed transport below threshold one expects that CASIM will underestimate “hits” caused by, say, (n, γ) interactions. The electromagnetic thresholds in CASIM for these calculations were 0.1 MeV for photons and 0.5 MeV for electrons. By contrast, MARS is capable of transporting low energy neutrons, although with presumably less precision than codes such as MCNP. The MARS thresholds were .002 eV for neutrons, 14.5 MeV for charged hadrons and 0.2 MeV for electrons and photons.

The “detectors” in the simulations were also quite different. In the CASIM calculations, The detector considered is two simple tracking chambers filled with Argon gas. Each chamber is 4 cm. thick in the beam direction, one being located 2m into the detector region and the other 4m into this region. The only other materials present are a 0.16 cm. thick steel beam pipe and g-10 “frames” on both of the chambers which are about 3 cm. thick radially. This is clearly a very *thin* detector. In general the expectation would be that higher fluences would exist in thicker (more realistic) detectors where, for example, more electromagnetic cascade build-up would occur. By contrast, the “detector” in the MARS calculations consisted of three slabs of material beginning 5m into the detector region. The first slab was 20 cm. thick (in the beam direction) CH, which was followed by a 20 cm. of Fe and a 400 cm. of CH. All of these extended to $R = 0$, forming a “beam dump” (although perhaps not a good one) for secondaries. Clearly this is a very *thick* detector. Thus, from both the physics capabilities and geometries considered, a higher fluence is expected from the MARS estimates when compared to those using CASIM.

The details of the results are presented elsewhere for both the MARS [8] and CASIM [9] calculations. As mentioned in Section I, the fluence is strongly dependent on location within the detector volume. As a simple characterization of the results, if one averages the results for a source location on either side of the Q3 magnet, then the maximum fluence found in the two detectors is:

MARS	$\sim 2.5 \times 10^{-2}$ charged particles/cm ² per Au ion
CASIM	$\sim 3.0 \times 10^{-3}$ charged particles/cm ² per Au ion

In both cases, the statistical error is significant, about 50%. In view of the remarks above the order of magnitude difference in these results is not unexpected. In any event, a “real detector” is more to the point, but has not been considered to date.

For the purposes of the estimation here, the geometric mean is probably appropriate, so a fluence of 9.0×10^{-3} charged particles/cm² per locally interacting Au ion will be used. Before leaving this section, it should be noted that the high β quadrupoles, which are the interaction points of the outscattered beam particles, are shielded (both physically and magnetically) from the detector region by the D0 and DX magnets. This aspect of the RHIC lattice makes it intrinsically more immune to halo background than other colliders where the high β quadrupoles are immediately upstream of the interaction regions.

V. Estimate of Background Levels

With the results given in the preceding sections (and subject also to the uncertainties as noted), an estimate of the maximum singles rate can be made if one knows “N”, the number of particles incident on the collimator per second. Now in fact N is unknown. For the purposes of obtaining an upper limit we assume that the calculated maximum rate of loss of Au ions due to Intra Beam Scattering, 5% per hour [10],⁶ is incident on a collimator. With this assumption, the components of Eqn. (1) at design intensity become:

$$N = \frac{.05 \times 57 \times 10^9}{3600} = 7.9 \times 10^5 \text{ ions / sec}$$

$$(1 - \epsilon) = 0.05$$

$$P = 0.5 \text{ local interactions (Worst Case IR)}$$

$$F = 9 \times 10^{-3} \text{ hits/cm}^2 \text{ per interaction}$$

$$\text{Total singles rate (Max)} = 180 \text{ hits/cm}^2\text{-sec.}$$

⁶This loss is from longitudinal phase space. The assumption that this loss somehow becomes a betatron loss is an extreme one.

The number, by itself, is not too informative. As an example consider the STAR TPC, a relatively slow device which has a “live time” of about 50 μsec . The above number translates to .009 background hits per cm^2 . This is to be compared to the hit density for charged tracks from a beam-beam collision which is given by:

$$\frac{\frac{dn}{dy}(ch)}{2\pi R^2}$$

For a central Au-Au collision, dn/dy is expected to be ~ 900 . At the TPC inner radius of 50 cm, this would be .057, a factor of over 6 higher than the maximum background hit density obtained above. On the other hand, at a radius of 1.27m the good track hit density becomes equal to the background hit density. This observation illustrates that the singles rate is overly simplistic as a measure of background. In this example, the real question is how the presence of background hits influences track reconstruction, which is well beyond the scope of this note. Clearly a detailed simulation of a “real detector” is needed to properly evaluate the effect of background. However, the simple singles rate estimated, which is believed to be a reasonable estimate of worst-case conditions, is not an obvious cause for alarm.

One of us [9] has compared beam halo to background from beam-gas interactions in the upstream Q3-Q4 regions. This comparison was made using CASIM and the “thin” detector described in the last section. The result, assuming a 10^{-9} Torr vacuum in the Q3-Q4 “warm” region and slightly adjusting the normalization in Ref. [9] to agree with the numbers presented here, is that the background hit rate from beam-gas collisions is higher than beam halo by a factor of 2.⁷ This is a very surprising result in view of the fact that the halo interactions are much closer to the detector region and that the rate of halo interactions is believed to be an upper limit. It stems in part from the observation made at the end of Section IV above that the D0 and DX magnets provide shielding for halo interactions in the upstream high β quadrupoles. What appears to be the opposite effect is at work in the case of beam-gas interactions, namely that the lattice is designed to transmit beam-like particles. In the model used in Ref. [9], forward spectator α particles are created in abundance in the beam-gas interactions and differ from the Au beam just enough to have a high probability of interacting on the beam pipe in the detector region or immediately upstream of the detector region. Since this conclusion depends on a specific fragmentation model it may not actually be true, but again serves to illustrate the importance of determining the source of background which actually bothers real detectors, which cannot be done prior to the existence of both machine and detectors.

VI. Summary

Combining a heuristic model of machine halo growth with simulations of outscattering from a limiting aperture collimator, lattice tracking, and hadron cascade calculations allows an

⁷ Since CASIM and the thin “detector” was used for both calculations, the halo singles rate is a factor of 3 lower than estimated in the text.

estimate of singles rate from machine halo in a “generic” detector, which is taken to be the zeroth order approximation of machine background. For Au beams an upper limit for this rate of ~ 180 hits/sec/cm² is obtained by assuming that the loss rate of Intra Beam Scattering is the halo source. This rate is comparable to estimates of beam-gas background. Although this estimate does not present an obvious problem, a host of systematic uncertainties, including the adequacy of characterizing background by such a simple quantity, would suggest that further studies be postponed until at least some of those uncertainties are resolved by the existence of a real machine and real detectors.

References

- [1] L. Burnod and J.B. Jeanneret, *Transverse Drift Speed Measurement of the Halo in a Hadron Collider*, Proceedings of the Workshop on Advanced Beam Instrumentation, KEK, P. 375 (1991). See also W. Fischer, M. Giovannozzi and F. Schmidt, *Dynamic Aperture Experiment at a Synchrotron*, Phys. Rev. E, Vol. 55, No. 3, p. 3507 (1997). [The latter reference describes a 10 year series of studies carried out at CERN.]
- [2] A. Van Ginneken, *ELSHIM, Program to Simulate Elastic Processes of Heavy Ions*, BNL-47618, AD/RHIC-100, Informatl Report (1992); and *Elastic Scattering in Thick Targets and Edge Scattering*, Physical Review D, Vol. 37, No. 11, p. 3292 (1988).
- [3] L. Schachinger and R. Talman, *A Thin Element Accelerator Program for Optics and Tracking*, SSC Central Design Group, Internal Report SSC-52 (1985).
- [4] M. Seidel, *The Proton Collimation System of HERA*, Dissertation, DESY 94-103 (1994).
- [5] S. White, Ed., *2nd Workshop Machine Backgrounds at RHIC*, Brookhaven National Laboratory 1996 (unpublished). Presentation by Dejan Trbojevic.
- [6] A. Van Ginneken, *CASIM; Program to Simulate Hadron Cascades in Bulk Matter*, Fermilab FN-272 (1975).
- [7] N.V. Mokhov, *The MARS Code System User's Guide Version 13*, Fermilab FN-628 (1995).
- [8] S. White, Ed. (Ref. [5]), Presentation by Pat Thompson.
- [9] A. J. Stevens, *Estimates of Beam-Gas Background Rates from Upstream Source Locations in a Simple Detector*, RHIC/DET Note 22 (1996).
- [10] J. Wei, private communication.

Calculated Single Pass Scraping Inefficiency

(45 cm. scraper - scraping at 5.5 sigma)

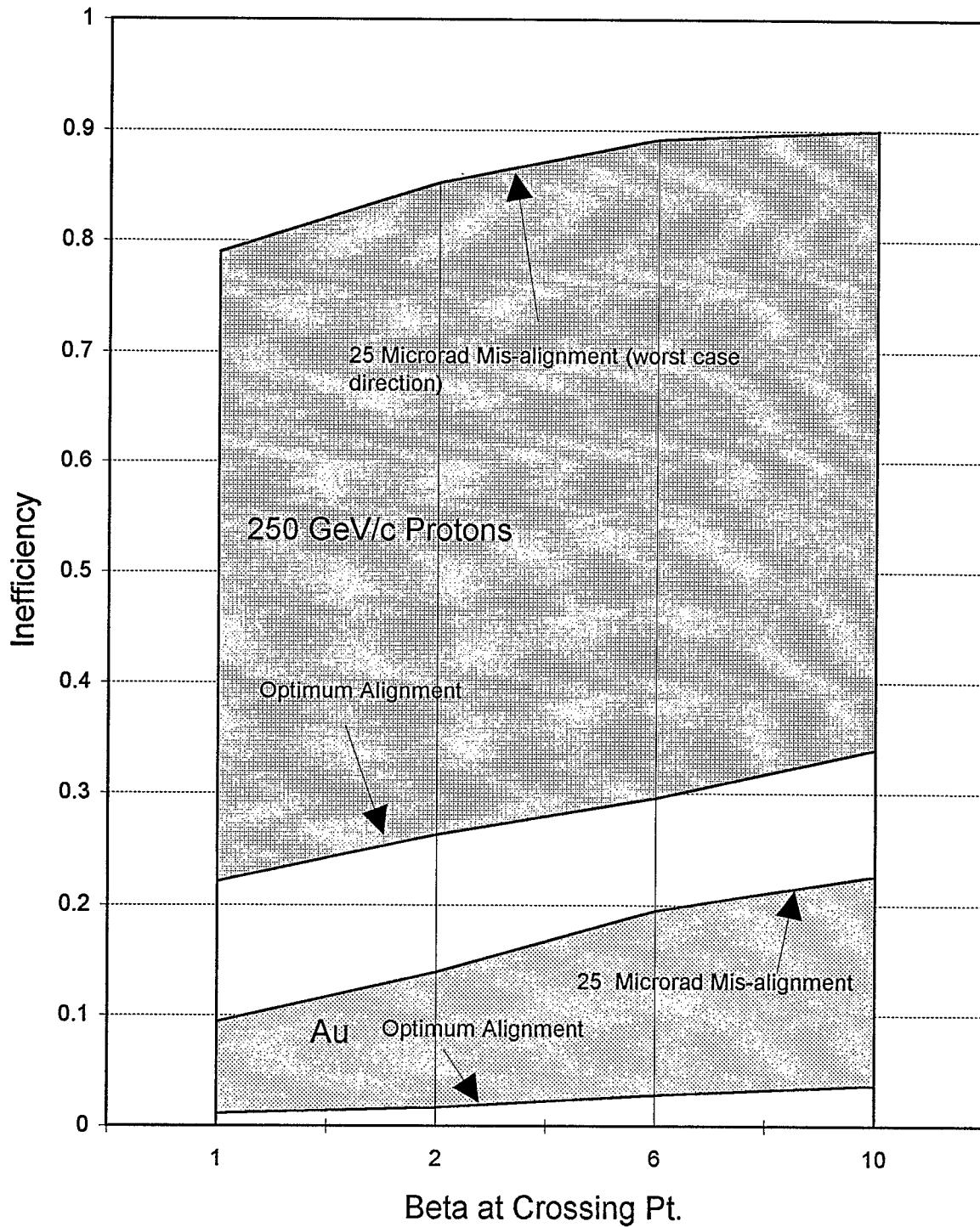


Fig. 1

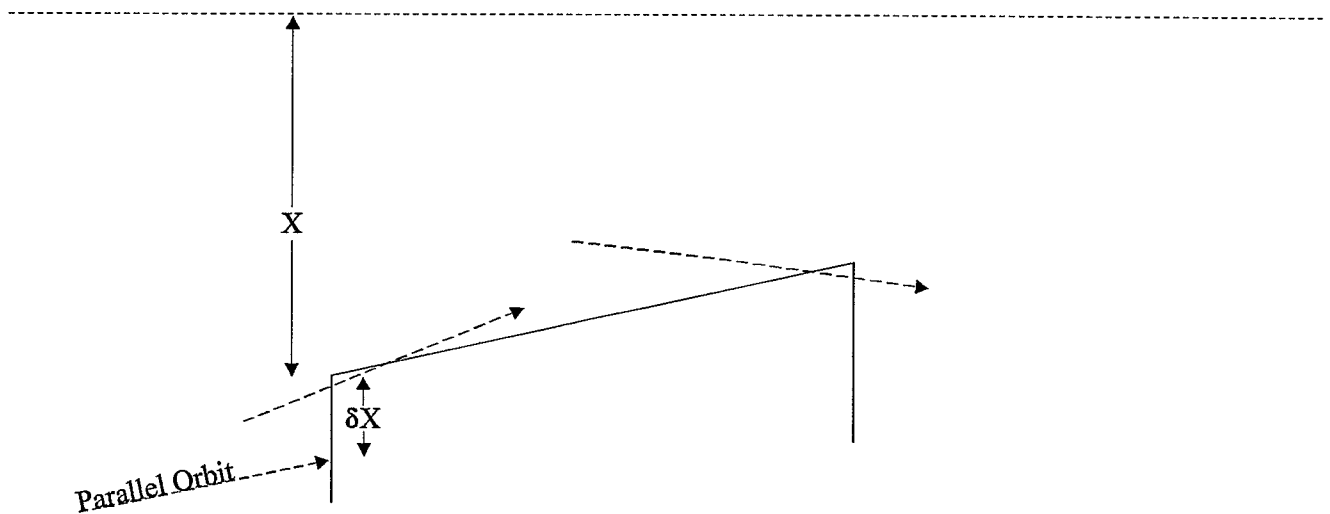
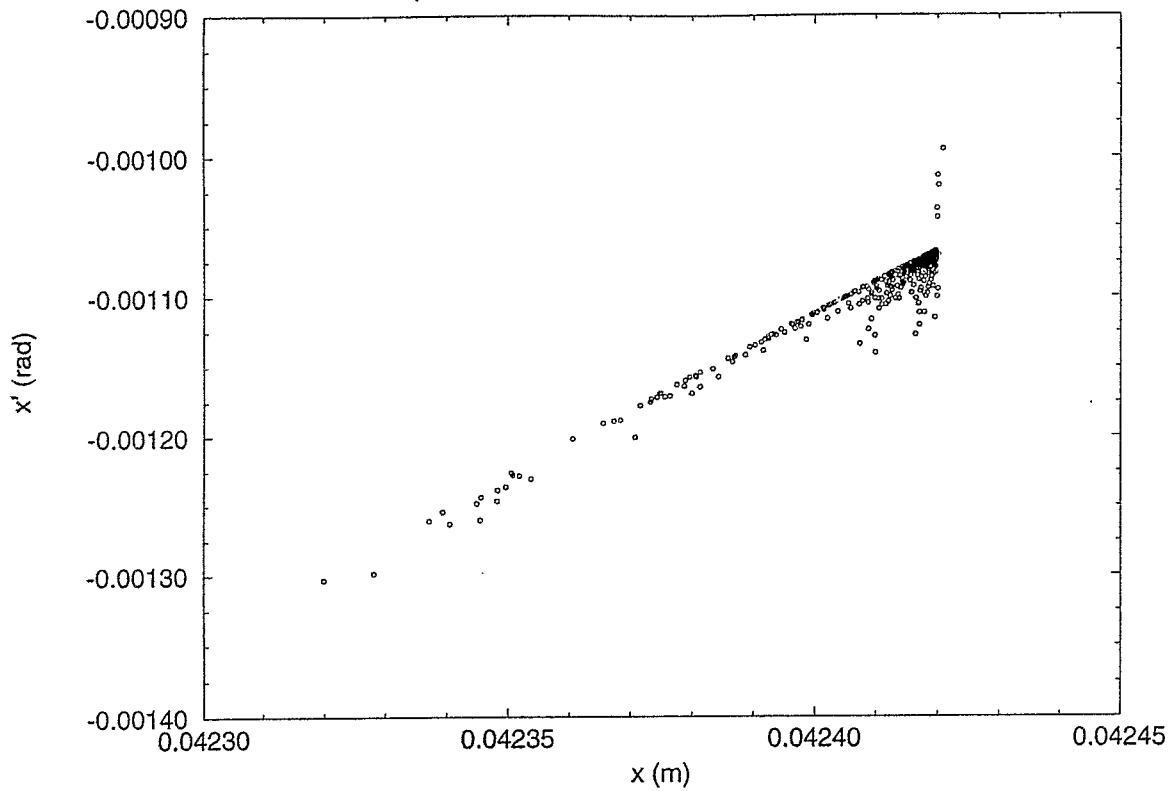


Illustration of halo particles encountering a limiting aperture collimator. Maximum scraping efficiency is achieved for "parallel orbits" where particles are at the maximum of their betatron oscillation. The sketch is not to scale. In the numerical simulation described in the text, δX is typically a few microns.

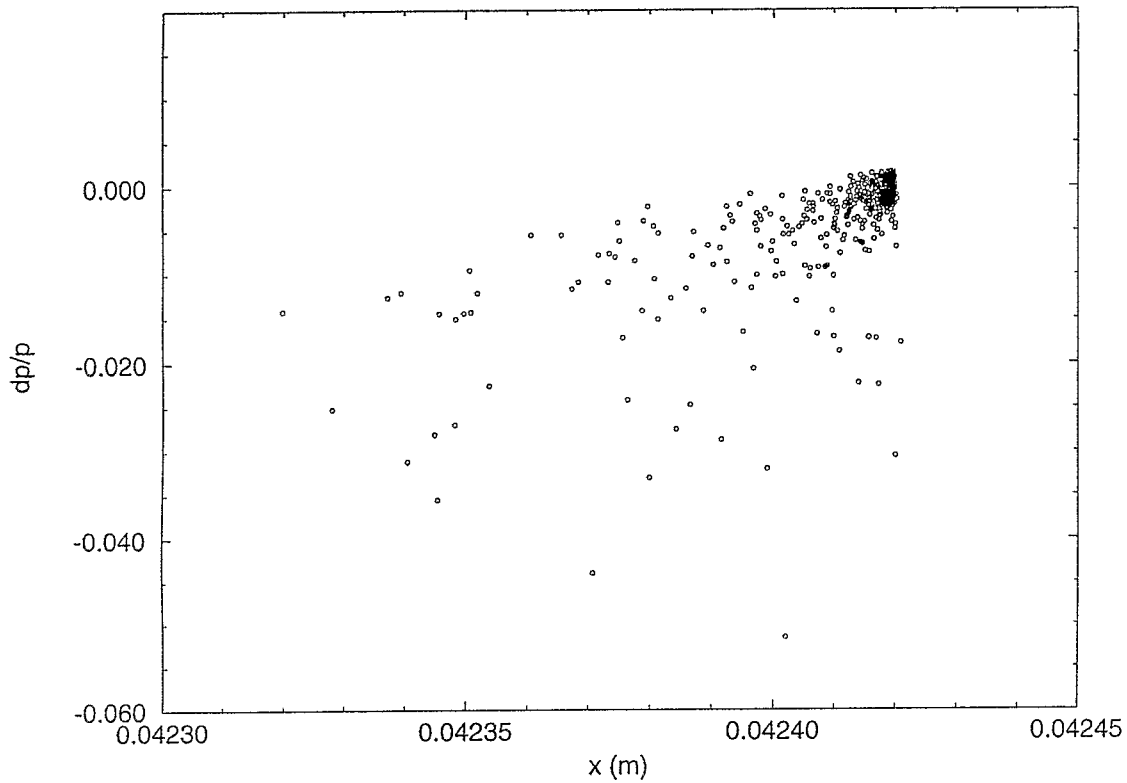
Fig. 2

Initial Distribution at the Primary Collimator
 $\beta = 1\text{ m @ 6 and 8 o'clock, } 10\text{ m at the rest}$



(a)

Initial x - dp/p Distribution at the Primary Collimator
 $\beta = 1\text{ m @ 6 and 8, } 10\text{ m at other IR}$



(b)

Fig. 3

Losses Around the Ring - TRACK -> initial condition abls. offsets
 Lattice: $\beta^* = 1\text{m}$ @ 6 and 8, 10m rest - Primary Collimator at 8 o'clock

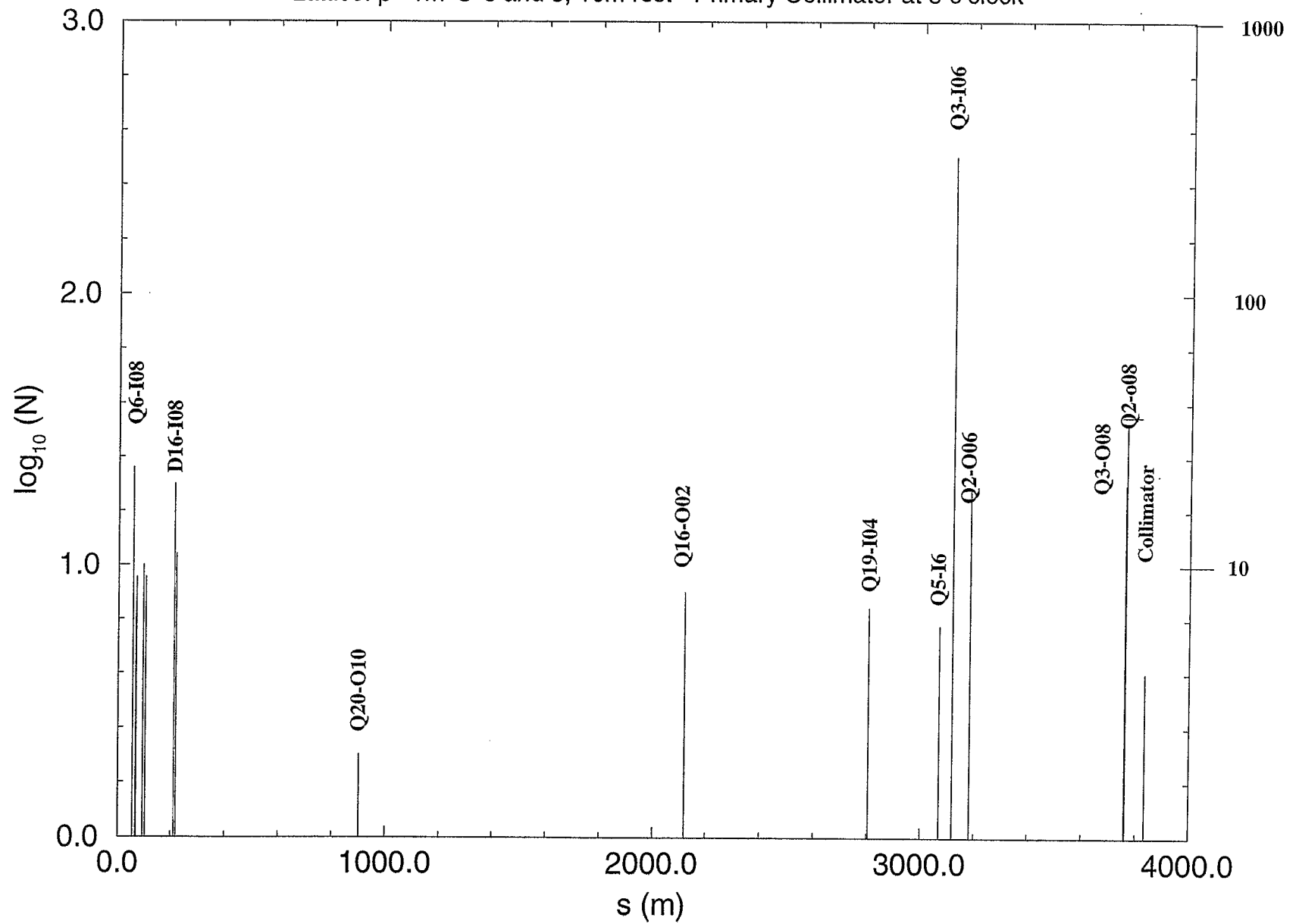


Fig. 4

Losses Around the Ring - Yellow Ring, set $\beta^* = 1\text{m}$ @ 6 and 8, 10 m rest
 Primary Collimator at 8 o'clock

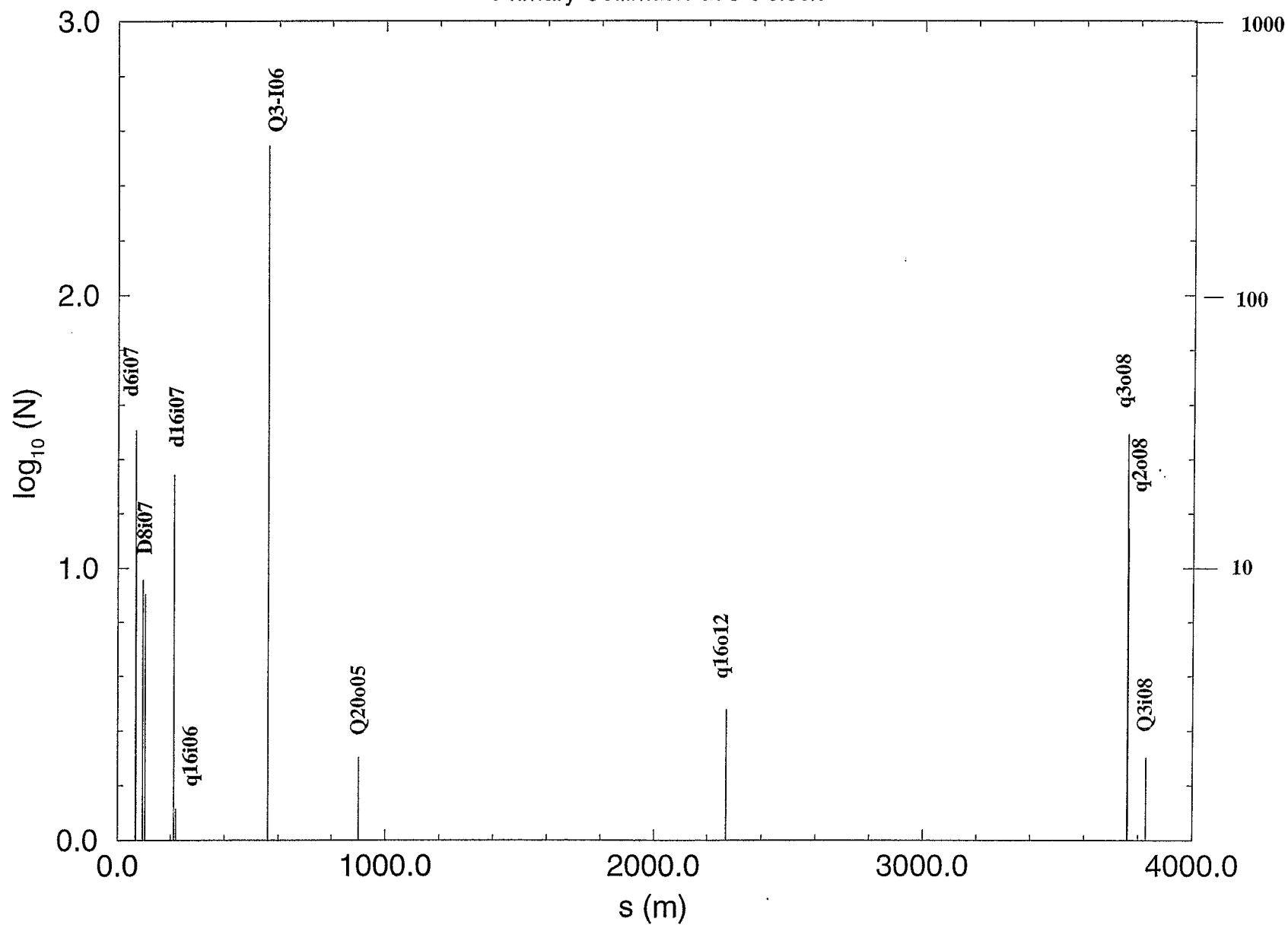


Fig. 5

Losses Around the Ring - TRACK \rightarrow initial condition abls. offsets
 Primary Collimator at 8 o'clock - Lattice $\beta^* = 1\text{m}$ @ 6 and 8, 2m @ 12

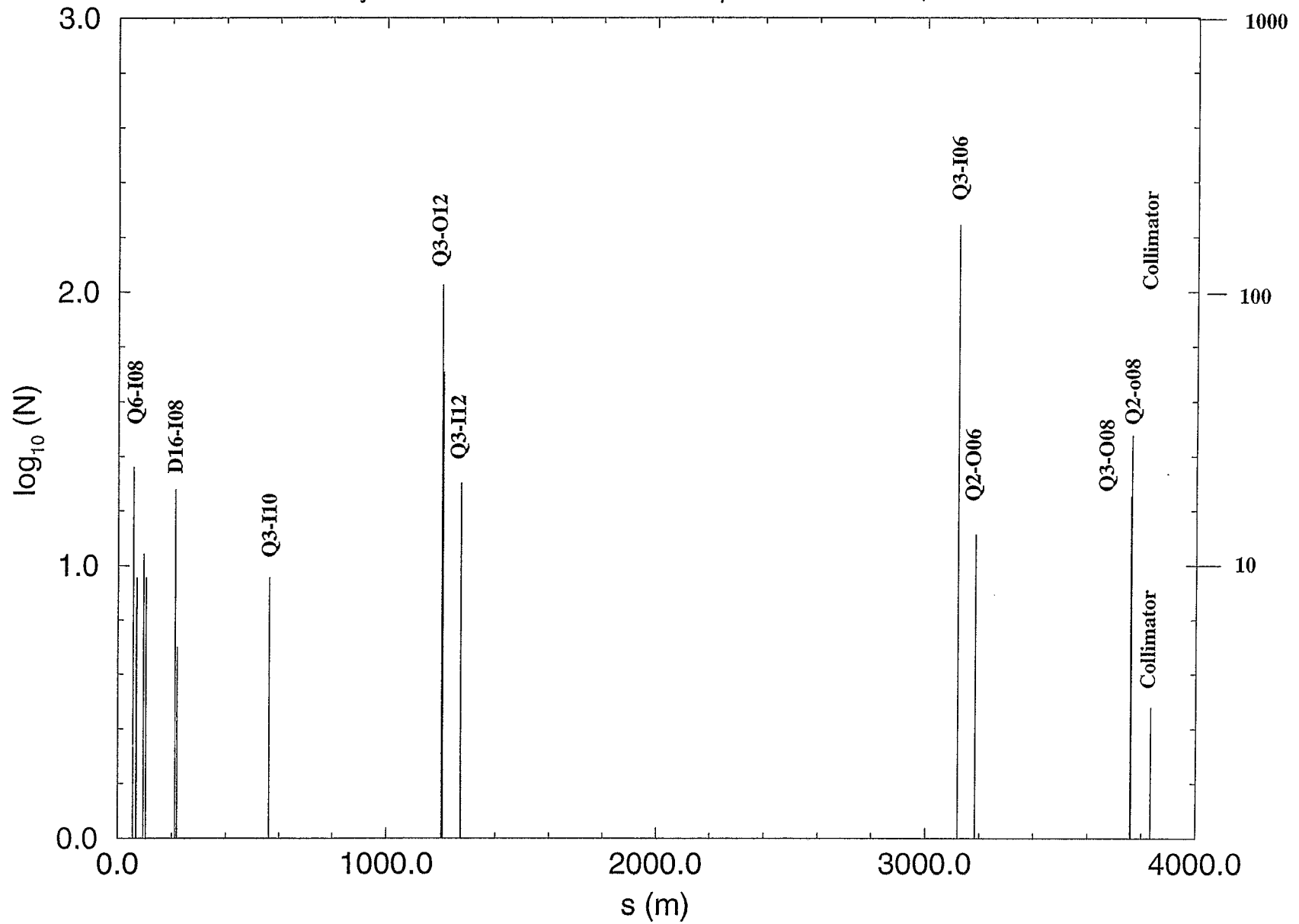


Fig. 6